USING ENVISAT SCANSAR DATA FOR CHARACTERISING SCALING PROPERTIES OF SCATTEROMETER DERIVED SOIL MOISTURE INFORMATION OVER SOUTHERN AFRICA

Daniel Sabel[(1)], Carsten Pathe[(1)], Wolfgang Wagner[(1)], Stefan Hasenauer[(1)], Annett Bartsch[(1)], Claudia Künzer[(1)], Klaus Scipal[(2)]

[(1)]Institute of Photogrammetry and Remote Sensing, Technical University of Vienna, Gusshausstrasse 27-29, 1040 Vienna, Austria, Email: ds@ipf.tuwien.ac.at
[(2)]European Centre for Medium-Range Weather Forecasts (ECMWF), Shinfield Park, Reading, RG2 9AX, United Kingdom, Email: Klaus.Scipal@ecmwf.int

ABSTRACT

Spaceborne scatterometers and radiometers offer soil moisture information with resolutions in the order of a few tens of kilometres. However, hydrologic users often request a resolution in the order of 1 km. Based on the insight that surface soil moisture in part is driven by large scale atmospheric forcing, a temporal analysis was carried out between backscatter on a local (1 km) and a regional (25 km) scale. The resulting scaling layer consist of the coefficient of determination between the two scales, which can be interpreted as the amount of soil moisture variation on the local scale explained by the variation of soil moisture on the regional scale. On locations where a high correlation is achieved, the regional soil moisture information, corresponding to scatterometer derived estimates, can be used directly on the 1 km scale. In agreement with theory, the highest correlations were found over agricultural fields and grasslands.

1. INTRODUCTION

Soil moisture, as a property and process occurring at the land-atmosphere boundary, is highly variable in space and time. Within a few meters soil moisture can vary as much as within a distance of kilometres [1] . Spatial soil moisture patterns usually follow topography, vegetation cover, land use or geological substrates, which are closely connected to the soil texture and water holding capacity [2] . In the temporal domain the moisture content in the uppermost centimetres of the soil profile, which is directly exposed to the influences of the atmosphere, can vary in the order of a few hours [3]. Several studies showed that soil moisture variations in time and space can be addressed to two different scale components – a small scale and a large scale component. The small scale component leads to local variations in soil moisture due to soil properties, land cover attributes and local topography. This small scale component acts in the range of tens of meters spatially and in the range of a few days temporally ([4], [5]). The large scale component is addressed to atmospheric forcing due to precipitation and evaporation processes [5] . Based on extensive in-situ data sets in Russia, [6] observed spatial correlation lengths of soil moisture in the order of 400 – 800 km caused by atmospheric forcing. These findings are supported by [7] , reporting spatial correlation lengths in the order of several hundred kilometres for test sites in Russia, Mongolia, China and Illinois, USA. But precipitation also occurs at different space and time scales. When looking at Figure 1, it can be seen that convective precipitation is a small scale phenomenon in the range of minutes to hours. Precipitation caused by frontal systems affect much wider areas, comprising spatial scales up to 1000 km and temporal scales from hours to days. Therefore, the mentioned large scale process is mainly affected by precipitation events in connection with moving frontal systems.

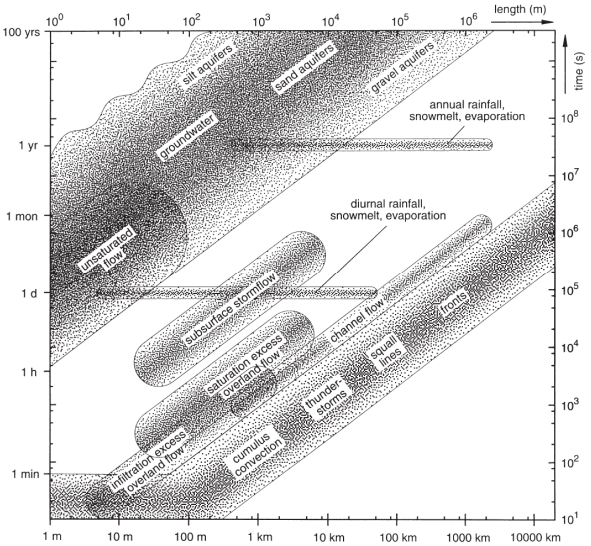

Figure 1: Temporal and spatial process scales in hydrology [8] .

Different studies has shown that coarse resolution soil moisture time series, representing an area more than 1000 km^2, and *in-situ* measurements of soil moisture, typically representing an area of 0.01 km^2 or less, can exhibit a strong correlation, despite the significant difference in spatial scales. Reference [9] found a

correlation of $R = 0.57$ between ERS scatterometer derived relative surface soil moisture time series and point measurements of top horizon soil moisture in Tibet. Other studies have produced similar results, e.g., [10] and [11] . The impact of atmospheric forcing on spatio-temporal soil moisture patterns explains, why in-situ soil moisture measurements, although representing point measurements, can be compared to regional representations of soil moisture. The correlation between scales is commonly described by means of a temporal stability analysis. The temporal stability concept was introduced by [12] as a tool for determining representative soil moisture measurement stations within a region. The behaviour can be described by the linear correlation coefficient between time series data of local soil moisture at the measurements sites and regional averages of soil moisture of all stations within a test site.

Based on the fact that changes in soil moisture have a strong influence on radar backscatter and therefore are reflected in radar backscatter time series data, the central idea of the temporal stability concept has been applied to ENVISAT ASAR GM data. Instead of comparing time series data of single soil moisture stations to regional soil moisture averages, single ASAR GM backscatter measurements called 'local backscatter' are compared to regional averages of ASAR GM data, called 'regional backscatter'. The spatial dimension of the region is oriented on the typical footprint size of microwave scatterometers.

Within the SHARE project, funded by ESA through the TIGER innovator programme, an automated processing chain for producing the scaling information was implemented. A scaling layer image was produced over southern Africa. In a first analysis, the influence of land cover was evaluated.

2. DATASET AND METHOD

2.1. Dataset

The scaling information was derived from ENVISAT's Advanced Synthetic Aperture Radar (ASAR) sensor in Global Monitoring Mode (GM). The ASAR sensor is operated at a frequency of 5.331 GHz (C-band). In GM mode, data is acquired with a resolution of 1 km. Due to the relatively low resolution, resulting in low power consumption, a potential duty cycle of 100% is achieved. The ScanSAR technique is facilitated through electronic beam steering, allowing a swath width of 405 km. Global coverage can be achieved within a few days, making ASAR GM data suitable for monitoring dynamic land processes.

2.2. Geocoding

The goal of the geocoding procedure was to achieve an accuracy of about half the pixel resolution (i.e. 500 m) using just the obit information from ENVISAT. This was achieved with the Range Doppler approach implemented using the geocoding routines of the SARscape software (by SARMAP). DORIS Precise Orbit State Vectors was used as orbit information input to the geocoding process.

2.3. Resampling

About 2300 images (as of Feb. 2007), totalling approximately 160 GB, were geocoded for the southern part of the African continent.

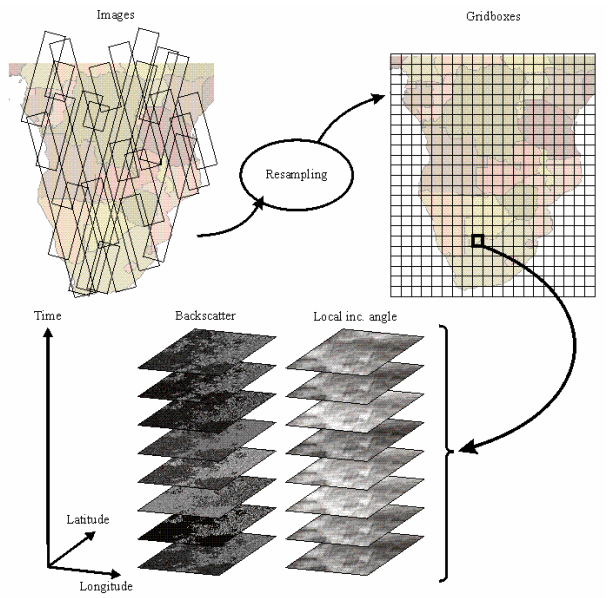

Figure 2: The resampling routines extract the data from many separate radar images and create a new database in an ordered grid.

Since subsequent processing steps were based on both spatial and temporal analysis, a resampling to a fixed grid in a new database format was required. The resampling routines were implemented using the IDL (Interactive Data Language) software from ITT. The backscatter amplitude and local incidence angle data from all images over a region were resampled to the new grid (see Figure 2) using bilinear interpolation. The 15 arc-seconds grid was divided into blocks of 0.5°x0.5° boxes (denoted "gridboxes"), resulting in 720 columns and 360 rows globally, to be used for efficient referencing of the data. The resampled data, i.e., backscatter intensity and local incidence angle, for each gridbox was stored in a separate file.

2.4. Normalisation

Radar backscatter generally shows a strong dependency on the local incidence angle. This effect is more pronounced in SAR imagery covering large incidence angle ranges like airborne SAR or spaceborne ScanSAR. Data acquired using the ScanSAR modes of the ENVISAT ASAR sensor are covering a much wider swath than conventional strip map mode SAR images like ERS-1/2 or ENVISAT ASAR Image Modes. ASAR GM data are covering incidence angles usually ranging from 20° to 40°.

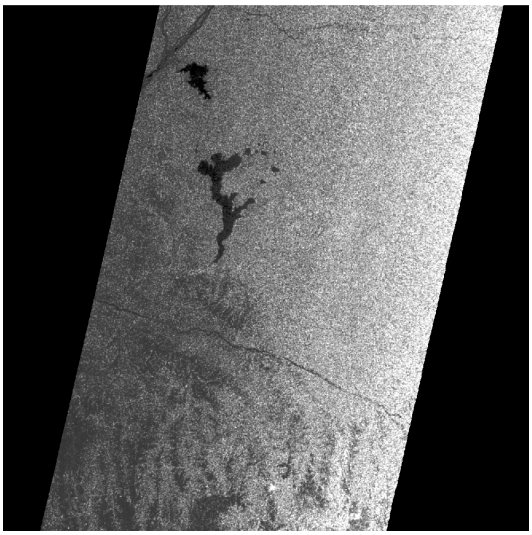

Figure 3: Decrease of radar image brightness from near range to far range in one ENVISAT ASAR GM scene due to the influence of the local incidence angle.

This causes a typical and consistent decrease in image brightness from near to far range, as exemplified in Figure 3. A linear relationship between the radar backscattering coefficient and the local incidence angle was observed. Figure 4 shows an example of the relation between the backscattering coefficient σ^0 and the local incidence angle θ for one grid location before normalisation. A linear dependence of the radar backscattering coefficient is also documented for Radarsat data by [13] and for ERS scatterometer data by [14] .

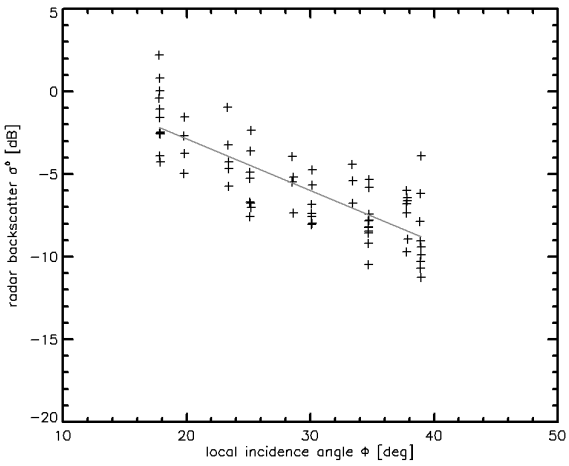

Figure 4: Radar backscattering coefficient σ^0 versus local incidence angle θ.

To remove the influence of local incidence angle on radar backscatter from ERS SAR, ERS scatterometer and RADARSAT data, linear models were fitted to the radar data to calculate backscatter values which are adjusted to predefined reference angles. Accordingly, the backscatter at each grid location was normalised to a reference angle of 30° according to Eq. 1 [15] .

$$\sigma^0(30) = \sigma^0(\theta) - a(\theta - 30) \qquad (1)$$

The parameter *a* is the slope of the fitted regression line.

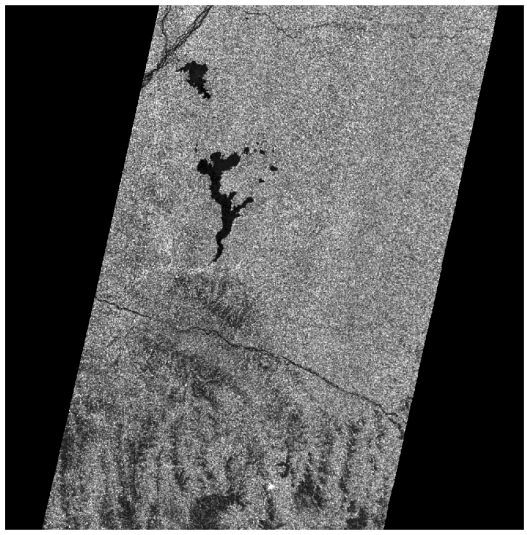

Figure 5: ASAR GM backscatter over the same area as in after incidence angle normalisation.

After normalisation the backscatter dependency on the local incidence angle is removed. Figure 5 show the same region as in Figure 3 after normalisation was applied.

2.5. Correlation

For each pixel in the 15 arc-second grid of the study area, the time-series of local backscatter values and the corresponding time-series of simultaneous regional backscatter were extracted. Data spanning the entire sensors lifetime (December 2004 – December 2006) were used. Typically, data from between 90 and 160 dates could be extracted for each location. The regional backscatter values were generated by averaging the backscatter over a 25x25 km window, centred on the position where the local backscatter was extracted. Equal weight was given to each measurement in the window. The relationship between the two data sets was then analyzed (Figure 6). The main result is the Pearson correlation coefficient, which quantifies the linear temporal consistency between the local and regional backscatter intensities. Several quality indicators, such as the number of measurements used and the fractional data coverage in the regional window, were also produced, to give a measure of the quality of the resulting information.

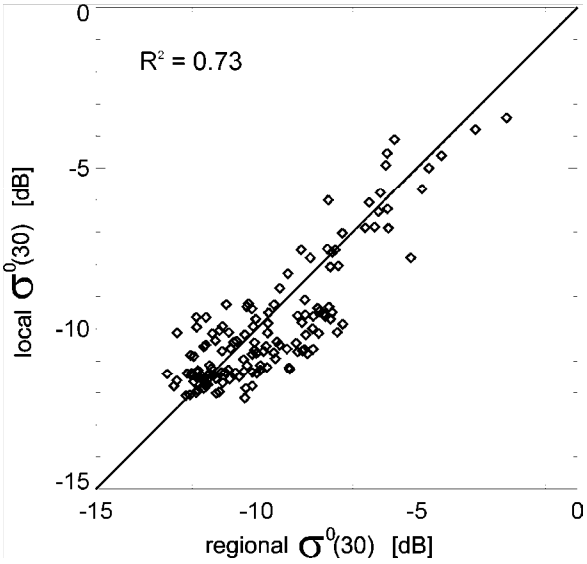

Figure 6: Example of scatterplot between regionally averaged backscatter and local backscatter.

3. RESULTS

The scaling layer (see Figure 7) contains the coefficient of determination (R^2), which was formed by taking the square of the Pearson correlation coefficient. R^2 can take on values between 0 and +1 and gives a measure of the amount of local backscatter variation explained by the backscatter variation on the regional scale.

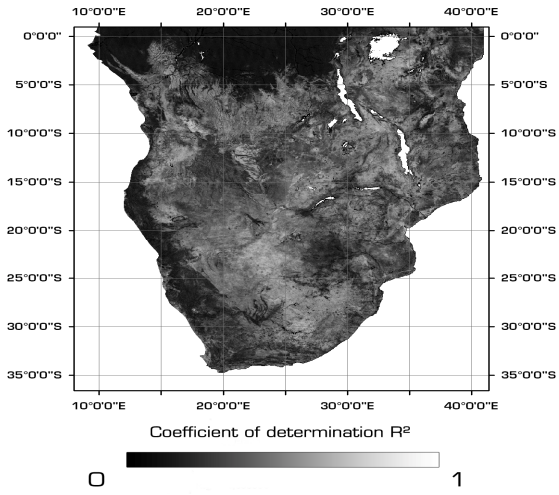

Figure 7: Coefficient of determination between local and regional backscatter intensity over the study area. Bright areas correspond to high correlation. Water bodies has been masked out.

Land cover features are clearly discernible, e.g., the low correlation of the Congo rainforest in the upper left part of the image (Figure 7). Large lakes, rivers and reservoirs have been masked out, and are displayed as homogeneous white areas, e.g., Lake Victoria to the east of the rainforest. Overall, large sections of the African continent show R^2-values above 0.55 [15] .

It was expected that land cover would have a prominent influence on the scaling layer. Using USGS Global Land Cover Characterization, the coefficient of determination was extracted for urban areas, agricultural fields, grassland, forest and barren land. The cumulative frequency histograms for each category are shown in Figure 8. It can be seen that high correlations were achieved for agricultural fields and grasslands. Forest, urban areas and barren land, which include areas with sparse or nonexistent vegetation such as deserts, salt flat and bare exposed rock, show low correlation. Agricultural fields and grasslands cover 68.9% of the study region.

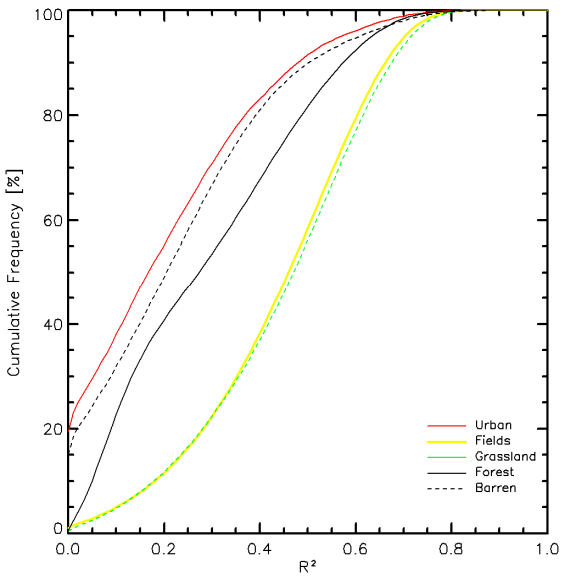

Figure 8: Cumulative frequencies of R² for different land cover classes.

4. DISCUSSION

Mainly three components influence radar backscatter, namely surface roughness, vegetation and soil water content. Large variations in surface roughness, e.g., ploughing of a field, are not likely to occur on a frequent basis at the 1 km or 25 km scale. Vegetation typically has an annual cycle of variation. It is proposed that soil water content, driven by atmospheric forcing, can explain a great part of the higher frequencies of variation recorded in the backscatter. Following this principle, it is assumed that the scaling layer also quantify the correlation between soil moisture variations on the two scales. Therefore, on locations where a high correlation is achieved, the regional soil moisture, corresponding to the scatterometer derived estimates, is also representative for the soil moisture content on the 1 km scale.

An important result of the correlation analysis is the fact that the relation between local and regional scale data in terms of land cover dependency is observed as expected. Over forest, volume scattering in the canopies often dominate over surface scattering from the soil surface. Therefore, a low response to changes in surface soil moisture is expected. Thus, a low correlation between the local and the regional backscatter variations is detected. In agricultural land and grassland, on the other hand, scattering in the surface layer of the soil contribute to a greater extent and therefore also the influence of soil moisture content in this layer has a more prominent impact on backscatter intensity. The result is stronger variations compared to forests or densely vegetated areas and thus also a higher correlation between scales.

5. CONCLUSION

ENVISAT ScanSAR data was used to characterise the applicability of coarse resolution soil moisture information, derived from scatterometers, on a finer spatial scale. This was done through the implementation of a scaling layer, which represents the temporal correlation between the backscatter intensities on a local (1 km) and a regional (25 km) scale. The scaling layer is an image consisting of the coefficient of correlation (R^2), which for each grid location gives a measure of the fraction of backscatter variation on the local scale explained by the backscatter variation on the regional (scatterometer) scale.

Using the scaling layer, it is possible to interpret the scatterometer derived soil moisture estimates on the local scale. It is predicted that downscaling will be possible over agricultural land and grassland, such as cropland, paste land and savanna. In accordance with theory, low correlation was achieved over forests and regions with nonexistent or sparse vegetation. In forest areas, the low correlation was attributed to the influence of canopy volume scattering, dominating any surface scattering contribution.

6. ACKNOWLEDGEMENTS

This study is a part of the development within the SHARE project, which is one of the European Space Agency's DUE Tiger projects. SHARE aims at enabling an operational soil moisture monitoring service for the southern and central regions of the African continent.

REFERENCES

[1] Dubayah, R., Wood, E.F., Lavallée, D. (1997): Multiscaling Analysis in Distributed Modelling and Remote Sensing: An Application Using Soil Moisture. *Scale in Remote Sensing and GIS*. D. A. Quattrochi and M. F. Goodchild. Boca Raton, Boston, London, New York, Washington, D.C., Lewis Publishers.

[2] Western, A.W., Blöschl, G. (1999): On the spatial scaling of soil moisture. *Journal of Hydrology* 217: 203-224.

[3] Raju, S., Chanzy, A., Wigneron, J., Calvet, J., Kerr, Y., Laguerre, L. (1995): Soil moisture and temperature profile effects on microwave emission at low frequencies. *Rem. Sens. Environ.* 54: 85-97.

[4] Entin, J.K., Robock, A., Vinnikov, K. Y., Hollinger, S.E., Liu, S., Namkhai, A. (1999): Temporal and spatial

scales of observed soil moisture variations in the extratropics. *J. Geophys. Res.* 105(D9): 11865-11877.

[5] Robock, A., Vinnikov, K.Y., Srinivasan, G., Entin, J.K., Hollinger, S.E., Speranskaya, N.A., Liu, S., Namkhai, A. (2000): The Global Soil Moisture Data Bank. *Bull. Amer. Meteorol. Soc.* 81: 1281-1299.

[6] Vinnikov, K. Y., Robock, A., Speranskaya, N. A., Schlosser, C. A. (1996): Scales of temporal and spatial variability of mitlatitude soil moisture. *J. Geophys. Res.* 101(D3): 7163-7174.

[7] Entin, J.K., Robock, A., Vinnikov, K. Y., Hollinger, S.E., Liu, S., Namkhai, A. (2000): Temporal and spatial scales of observed soil moisture variations in the extratropics. *J. Geophys. Res.* 105(D9): 11865-11877.

[8] Blöschl, G., Sivapalan, M. (1995): Scale Issues in Hydrological Modelling: A Review. *Hydrological Processes* 9: 251-290.

[9] Wen, J., Su, Z. (2003): A time series based method for estimating relative soil moisture with ERS wind scatterometer data. *Geophysical Research Letters* 30(7): doi:10.1029/2002GL016557.

[10] Wagner, W., Scipal, K., Pathe, C., Gerten, D., Lucht, W., Rudolf, B. (2003): Evaluation of the agreement between the first global remotely sensed soil moisture data with model and precipitation data. *J. Geophys. Res. Atmos.* 108(D19): 4611, DOI10.1029/2003JD003663.

[11] Bindlish, R., Jackson, T. J., Wood, E., Gao, H., Starks, P., Bosch, D., Lakshmi, V. (2003): Soil moisture estimates from TRMM Microwave Imager observations over the Southern United States. *Rem. Sens. Environ.* 85: 507-515.

[12] Vauchaud, G., Passerat de Silans, A., Balabanis, P., Vauclin, M. (1985): Temporal Stability of Spatially Measured Soil Water Probability Density Function. *Soil Science Society of America* 49: 822-828.

[13] Mäkynen, M. P., Manninen, T., Similä, M. H., Karvonen, J. A., Hallikainen, M. T. (2002): Incidence Angle Dependence of the Statistical Properties of C-Band HH-Polarization Backscattering Signatures of the Baltic Sea Ice. *IEEE Trans. Geosci. Rem. Sens.* 40(12): 2593-2609.

[14] Frison, P.-L., Mougin, E. (1996): Use of ERS-1 Wind Scatterometer Data over Land Surfaces. *IEEE Trans. Geosci. Rem. Sens.* 34(2): 550-560.

[15] Sabel, D. (2006). Scaling information for scatterometer derived soil moisture estimates. Master Thesis. Luleå University of Technology. ISSN: 1402-1617.